Chapter 1

SEMF and Neutron Stars

"The same short-range force that saturates $B/A \sim 8\,\mathrm{MeV}$ *cannot bind pure neutrons; only gravity at stellar mass can."*

after Weizsäcker; Bethe (SEMF)

1.1 The puzzle: pure neutrons fail on Earth

The SEMF was built for ordinary nuclei near the valley of stability. If one asks what happens for pure neutron matter, $Z = 0$, the volume and asymmetry terms no longer cancel in a favourable way: the nuclear terms alone leave pure neutrons unbound. Laboratory nuclei never form a stable drop of neutrons.

Nature nevertheless produces compact stellar remnants that are mostly neutrons in the bulk, with masses of order a solar mass and radii of order ten kilometres. Gravity, negligible on the fermi scale of a single nucleus, becomes the leading long-range attraction at $A \sim 10^{56}$–10^{57}. This chapter extrapolates the liquid-drop idea to that extreme and recovers the solar-mass, ten-kilometre scale of neutron stars as an order-of-magnitude estimate [1, 4, 6].

1.1.1 Nuclear landscape and the neutron drip line

Lecture 5 fixed the most stable Z at fixed A. The chart of nuclides (Figure 1.1; cf. Lectures 4–5) also shows, for each Z, a maximum N that still binds. Beyond that **neutron drip line**,

$$S_n(A, Z) = \left[M(A-1, Z) + m_n - M(A, Z)\right]c^2 \le 0, \tag{1.1}$$

and the last neutron is unbound (Lecture 4 separation-energy language). Even the dineutron is unbound; few-neutron systems are unstable. Protons, and the Coulomb–asymmetry balance of Lectures 4–5, are essential for ordinary nuclei.

From the SEMF alone, pure neutron matter ($Z = 0$, $N = A$) has

$$\frac{B}{A} \approx a_V - a_\mathrm{a} \approx 15.5 - 23 \approx -7.5\,\mathrm{MeV} < 0 \tag{1.2}$$

(neglecting surface for large A). Asymmetry wins: liquid-drop nuclear physics alone *forbids* a stable pure-neutron drop of any laboratory size.

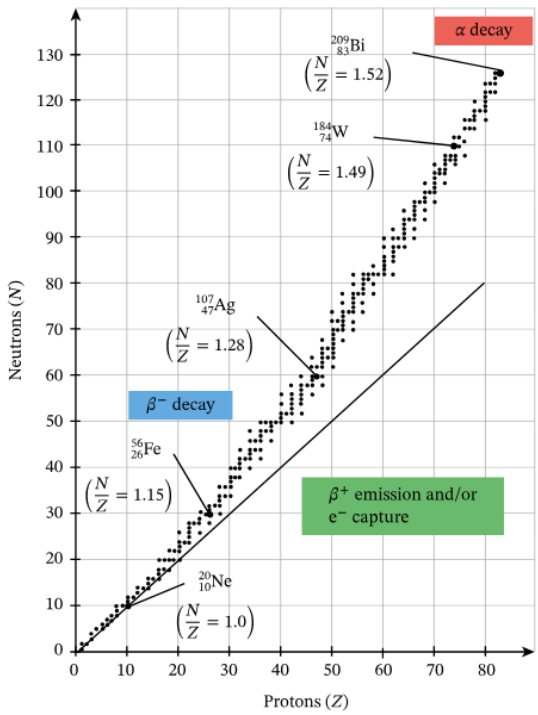

Figure 1.1: Nuclear landscape (valley of stability). For each Z only a limited band of N is bound. Beyond the neutron drip line, $S_n \leq 0$ and neutrons unbind. Laboratory nuclei never reach pure-neutron bulk matter.

1.1.2 Neutron stars exist anyway

Nature produces compact remnants that are mostly neutrons in the bulk (with a thin outer crust of nuclei and a small proton fraction in the core). Observed scales:

Quantity	Typical value
Mass	$\sim (1\text{–}2)\, M_\odot$
Radius	$\sim 10\text{–}15\,\text{km}$
Mean density	$\sim (1\text{–}3)\, \rho_0$ (nuclear saturation)
Nucleon number	$A \sim 10^{57}$ for $M \sim M_\odot$

That is $\sim 10^{55}$ times more nucleons than uranium, in a city-sized volume. The SEMF question: *how can such an object be bound when few neutrons are not?*

1.2 Birth of a neutron star

A compact sketch is enough for this nuclear course [4]:

1. Gas clouds collapse under gravity; fusion begins when the core is hot and dense (H $\to$ He in the Sun).

2. In stars several times heavier than the Sun, fusion proceeds through He, C, O, . . . up to the iron-group peak of B/A (Lecture 4). Fusion past iron does not release net energy.

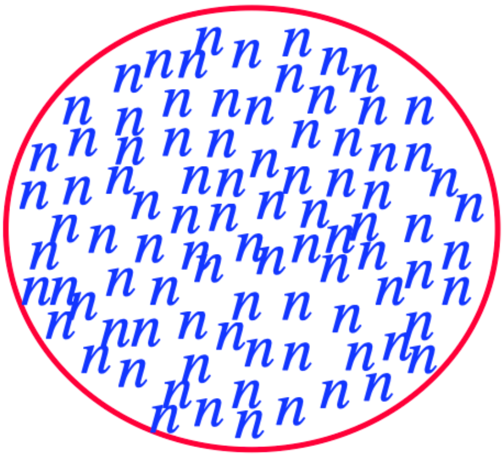

Figure 1.2: Schematic pure-neutron bulk (lecture cartoon). The star is not a giant laboratory nucleus: gravity and quantum degeneracy dominate the global energy and support balance.

3. When nuclear burning can no longer support the core, gravity wins: rapid collapse, bounce, and a core-collapse supernova that ejects the envelope.
4. In the residual core, electron Fermi energies become so high that inverse β decay (electron capture)

$$p + e^- \to n + \nu_e$$

converts most protons into neutrons. Neutrinos escape; the remnant cools into a neutron star.

Why inverse β wins at high density. In free space, $m_n c^2 - m_p c^2 \approx 1.3\,\mathrm{MeV}$ and free neutrons β^- decay. Inside a dense Fermi sea of electrons, capturing an electron from a high Fermi level can lower the total energy of the system even though the free n is heavier. The chemical potentials rearrange until β equilibrium

$$\mu_n = \mu_p + \mu_e \tag{1.3}$$

is reached, typically with a proton fraction of only a few percent in the core: *mostly* neutrons, not purely $Z = 0$.

1.3 Scales: density, number of neutrons, and forces

1.3.1 Number of nucleons

One solar mass is $M_\odot \approx 2 \times 10^{30}\,\mathrm{kg}$. With $m_n \approx 1.67 \times 10^{-27}\,\mathrm{kg}$,

$$A_\odot \approx \frac{M_\odot}{m_n} \approx \frac{2 \times 10^{30}}{1.67 \times 10^{-27}} \approx 1.2 \times 10^{57}. \tag{1.4}$$

A $1.4\,M_\odot$ neutron star therefore contains of order 10^{57} nucleons.

1.3.2 Mean density and the nuclear connection

Nuclear saturation density from Lectures 1–2 is

$$n_0 \approx 0.16\,\mathrm{fm}^{-3} = 1.60 \times 10^{44}\,\mathrm{m}^{-3}. \tag{1.5}$$

This is a *number* density. Multiplication by the nucleon mass gives

$$\rho_0 = m_n n_0 \approx (1.6749 \times 10^{-27}\,\mathrm{kg})(1.60 \times 10^{44}\,\mathrm{m}^{-3}) \approx 2.68 \times 10^{17}\,\mathrm{kg\,m}^{-3}. \tag{1.6}$$

If a star of mass $M = 1.4\,M_\odot$ has radius $R = 12\,\mathrm{km}$,

$$\bar{\rho} = \frac{3M}{4\pi R^3} \approx 3.8 \times 10^{17}\,\mathrm{kg\,m}^{-3} \approx 1.4\,\rho_0. \tag{1.7}$$

Neutron stars are *nuclear-density objects* writ large: the same saturation that fixed $R = r_0 A^{1/3}$ for Pb reappears as a kilometre-scale radius for $A \sim 10^{57}$.

One uniform-density radius, written two ways

For a uniform sphere, $A = n_0(4\pi R^3/3)$, so

$$R = \left(\frac{3A}{4\pi n_0}\right)^{1/3} = r_0 A^{1/3}, \qquad r_0 \equiv \left(\frac{3}{4\pi n_0}\right)^{1/3} \approx 1.14\,\mathrm{fm}.$$

For $A = 10^{57}$, both forms give $R \approx 11.4\,\mathrm{km}$. Using the rounded nuclear-size coefficient $r_0 = 1.2\,\mathrm{fm}$ instead gives $12\,\mathrm{km}$. These are the same uniform-density estimate, not independent radius prescriptions.

1.3.3 Why gravity was dropped in Lectures 4–5

For two nucleons a fermi apart,

$$\frac{Gm_n^2}{r} \sim 10^{-36}\,\mathrm{MeV} \qquad (r \sim 1\,\mathrm{fm}),$$

negligible next to a_V, a_C, or a_a. For $A \sim 10^{57}$ nucleons in a sphere of radius $\sim 10\,\mathrm{km}$, every nucleon feels the gravitational field of the whole star. Total gravitational self-energy scales as $GM^2/R \sim A^{5/3}$ at fixed density and can outweigh a fixed MeV-per-nucleon nuclear deficit.

Key idea

Laboratory nuclei: drop G. Neutron-star scale: keep G. The SEMF structure is reused as energy bookkeeping; gravity is the new long-range term.

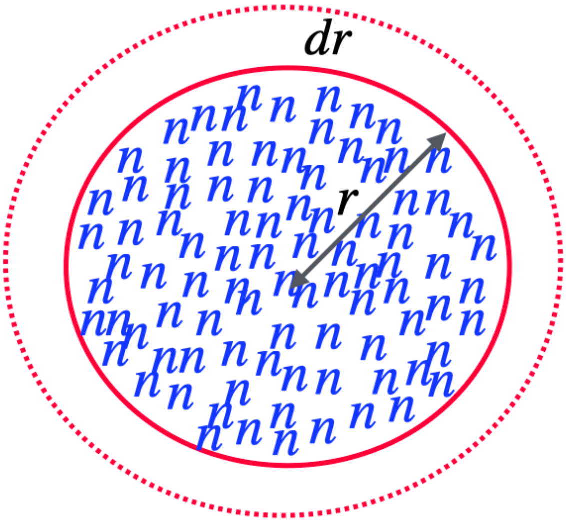

Figure 1.3: Assembly of a uniform sphere by thin shells. A shell of thickness dr at radius r feels the potential of the mass already inside r. Integrating gives $U_G = -3GM^2/(5R)$.

1.4 Gravitational self-energy of a uniform sphere

1.4.1 Derivation (same logic as Coulomb 3/5)

Uniform density $\rho = M/(\frac{4}{3}\pi R^3)$. Enclosed mass at radius r:

$$m(r) = M\,\frac{r^3}{R^3}. \tag{1.8}$$

Shell mass:

$$\mathrm{d}m = 4\pi r^2\,\mathrm{d}r\,\rho = \frac{3M}{R^3}\,r^2\,\mathrm{d}r. \tag{1.9}$$

Potential of the interior on the shell:

$$\phi(r) = -\frac{G\,m(r)}{r} = -\frac{GM\,r^2}{R^3}. \tag{1.10}$$

Work to bring $\mathrm{d}m$ from infinity:

$$\mathrm{d}U = \phi\,\mathrm{d}m = -\frac{3GM^2}{R^6}\,r^4\,\mathrm{d}r. \tag{1.11}$$

Integrate $0 \to R$:

$$U_G = -\frac{3GM^2}{5R}. \tag{1.12}$$

Compare with the Coulomb self-energy of a uniform charged sphere (Lecture 4):

$$E_\mathrm{C} = \frac{3}{5}\frac{k_e(Ze)^2}{R}, \qquad U_G = -\frac{3}{5}\frac{GM^2}{R}.$$

Same geometric factor 3/5; opposite sign because gravity is attractive.

Binding language. $U_G < 0$ lowers the total energy relative to dispersed matter at infinity. In nuclear $B > 0$ language (Lecture 4), gravity contributes $+|U_G| = 3GM^2/(5R)$ to the binding budget.

Physics checklist for Figure 1.3

1. Shell-by-shell assembly: identical strategy to electrostatics.
2. Scaling: $U_G \propto M^2/R \propto A^{5/3}$ at fixed density.
3. Real stars are stratified; the GM^2/R scaling remains the right order of magnitude.

1.5 A labelled toy model: SEMF plus gravity

1.5.1 Modified binding energy

This section is a **toy EOS/energy model**, not a microscopic equation of state for neutron-star matter. Start from the SEMF of Lectures 4–5 and add the magnitude of the Newtonian gravitational self-energy as an extra contribution to the *binding* energy (positive when the system is more tightly held together than free nucleons):

$$B = a_V A - a_S A^{2/3} - a_C \frac{Z(Z-1)}{A^{1/3}} - a_{\mathrm{a}} \frac{(N-Z)^2}{A} + \delta + \frac{3GM^2}{5R}. \tag{1.13}$$

In a total-energy ledger the gravitational self-energy is negative ($U_G = -3GM^2/5R$); writing $+|U_G|$ in B is the same physics packaged as binding. The pure-neutron SEMF exercise below uses this convention only as an order-of-magnitude cartoon.

1.5.2 Idealised pure-neutron limit

Take $Z = 0$, $N = A$, $M = m_n A$, and impose the same uniform density throughout:

$$R = r_0 A^{1/3}, \qquad r_0 = \left(\frac{3}{4\pi n_0}\right)^{1/3} \approx 1.14\,\mathrm{fm}.$$

- Coulomb vanishes;
- asymmetry: $-a_{\mathrm{a}}(N-Z)^2/A = -a_{\mathrm{a}}A$;
- surface $\propto A^{2/3}$ negligible vs volume for huge A (surface/volume $\to 0$; same reason bulk beats surface in macroscopic matter);
- pairing $\propto A^{-3/4}$ negligible at $A \sim 10^{56}$.

Then

$$\frac{3GM^2}{5R} = \frac{3Gm_n^2}{5r_0} A^{5/3}, \tag{1.14}$$

and

$$B \approx (a_V - a_{\mathrm{a}})\, A + \frac{3Gm_n^2}{5r_0} A^{5/3}. \tag{1.15}$$

Nuclear piece alone is negative.

$$a_V - a_{\mathrm{a}} \approx -7.5\,\mathrm{MeV}.$$

That is the SEMF version of "you cannot build a stable nucleus from neutrons alone."

Gravity can reverse the sign. The second term grows as $A^{5/3}$. For large enough A it overcomes the 7.5 MeV per-nucleon deficit.

Caution

What this calculation is and is not. It is a pedagogical SEMF extrapolation: an existence argument for a bound pure-neutron system at stellar A. It is *not* modern neutron-star structure. Real support against collapse is neutron **degeneracy pressure** (and nuclear repulsion at short distance) balanced by gravity in general-relativistic hydrostatic equilibrium (Tolman–Oppenheimer–Volkoff equation). Gravity is attractive; degeneracy provides the outward pressure. Here gravity enters only as extra binding in an energy ledger, good for order-of-magnitude A and M, not for precision $M(R)$ curves or the maximum mass.

1.6 Boundedness: critical A, mass, and numerical estimate

Require $B \geq 0$. Divide (1.15) by A:

$$(a_V - a_\mathrm{a}) + \frac{3Gm_n^2}{5r_0} A^{2/3} \geq 0. \tag{1.16}$$

With $a_V - a_\mathrm{a} \approx -7.5\,\mathrm{MeV}$,

$$A^{2/3} \geq \frac{7.5\,\mathrm{MeV}}{C}, \qquad C \equiv \frac{3Gm_n^2}{5r_0}. \tag{1.17}$$

Order of magnitude for C. In SI units,

$$\begin{aligned} G &= 6.67 \times 10^{-11}\,\mathrm{m^3\,kg^{-1}\,s^{-2}}, \\ m_n &= 1.67 \times 10^{-27}\,\mathrm{kg}, \\ r_0 &= 1.14\,\mathrm{fm} = 1.14 \times 10^{-15}\,\mathrm{m}. \end{aligned}$$

Then

$$\begin{aligned} \frac{Gm_n^2}{r_0} &= \frac{6.67 \times 10^{-11}\,(1.67 \times 10^{-27})^2}{1.14 \times 10^{-15}} \approx 1.63 \times 10^{-49}\,\mathrm{J} \\ &\approx 1.02 \times 10^{-36}\,\mathrm{MeV}, \end{aligned}$$

so

$$C = \frac{3}{5}\frac{Gm_n^2}{r_0} \sim 6 \times 10^{-37}\,\mathrm{MeV}.$$

Requiring $CA^{2/3} \gtrsim 7.5\,\mathrm{MeV}$ gives

$$A^{2/3} \gtrsim \frac{7.5}{6 \times 10^{-37}} \sim 1.25 \times 10^{37},$$

and raising both sides to the 3/2 power,

$$A \gtrsim \left(1.25 \times 10^{37}\right)^{3/2} = \left(1.25 \times 10^{37}\right)\sqrt{1.25 \times 10^{37}} \sim 10^{56}.$$

Thus

$$A \gtrsim 10^{56} \tag{1.18}$$

(lecture estimate; the prefactor depends on the exact gap $a_\mathrm{a} - a_V$ and on r_0).

Mass.

$$M \approx m_n A \sim 10^{56} \times 1.67 \times 10^{-27}\,\mathrm{kg} \sim 1.7 \times 10^{29}\,\mathrm{kg} \sim 0.1\,M_\odot$$

for $A \sim 10^{56}$. Using $A \sim 10^{57}$ (closer to observed $1\,M_\odot$) matches solar-mass neutron stars. The SEMF+gravity argument recovers the *solar-mass order of magnitude*: that is its success [4].

Why $A = 2$, 100, or even 10^{10} still fail

For any laboratory or even planetary A, the gravity term per nucleon is far below 1 eV. Then

$$\frac{B}{A} \approx a_V - a_\mathrm{a} < 0:$$

unbound. Only stellar A makes $CA^{2/3}$ competitive with 7.5 MeV.

Scale	A	Nuclear B/A	Gravity vs nuclear
Deuteron	2	$\sim +1.1\,\mathrm{MeV}$ (needs $p+n$)	irrelevant
Lead	~ 200	$\sim +8\,\mathrm{MeV}$	irrelevant
“Neutron drop” (lab)	any small	$\sim -7.5\,\mathrm{MeV}$ if $Z=0$	still unbound
Neutron star	$\sim 10^{57}$	nuclear + $\lvert U_G \rvert$	gravity decisive

1.7 Physics beyond the SEMF cartoon

1.7.1 What actually supports a neutron star

In hydrostatic equilibrium, gravity pulls inward and a pressure gradient holds the star up. For white dwarfs the pressure is electron degeneracy; for neutron stars it is primarily **neutron degeneracy pressure** (Fermi gas of neutrons at nuclear density), stiffened at high density by repulsive nuclear forces. The SEMF calculation never writes that pressure: it only asks whether the total energy is lower than that of dispersed nucleons. Both viewpoints are useful; they answer different questions (global binding vs local force balance).

1.7.2 Internal structure (qualitative)

- **Atmosphere / outer crust:** ordinary (exotic) nuclei in a lattice with electrons; density rises from $\mathrm{g\,cm^{-3}}$ toward nuclear.
- **Inner crust:** neutron-rich nuclei coexist with a neutron fluid (past the drip density).

- **Outer core:** uniform *npe* matter (neutrons, protons, electrons) in β equilibrium; mostly neutrons.
- **Inner core:** uncertain (hyperons? deconfined quarks?): the regime where laboratory SEMF coefficients are least trustworthy.

1.7.3 Link back to asymmetry and the Fermi gas

The same Pauli filling that produced the asymmetry term $-a_\mathrm{a}(N-Z)^2/A$ (Lecture 4) is the microscopic origin of Fermi kinetic energy. In pure neutron matter the kinetic energy per nucleon is large; the SEMF packages that cost into a_a. Gravity does not cancel the Pauli principle: it adds a different energy scale that grows with system size.

Key idea

SEMF alone: pure neutrons unbound ($a_V < a_\mathrm{a}$). SEMF + gravity: a bound system appears only for $A \gtrsim 10^{56}$, with $M \sim M_\odot$ and $R \sim 10\,\mathrm{km}$ as order-of-magnitude scales. Few neutrons cannot form a star; a stellar number of neutrons can. Realistic stars are not pure neutron and are not held by this energy ledger: they are charge-neutral, β-equilibrated matter supported by an equation of state in hydrostatic (TOV) equilibrium.

1.8 Lessons and course connection

1. Asymmetry energy is real: unbound pure-neutron drops and the need for $N \sim Z$ in light nuclei share one SEMF term.
2. Coefficients a_V, a_a are terrestrial fits; using them at $A = 10^{57}$ is a bold but instructive extrapolation.
3. Gravity changes the ranking of terms: surface, Coulomb, and pairing drop out; volume, asymmetry, and GM^2/R remain.
4. Saturation density links fm and km: $R = r_0 A^{1/3}$ from electron scattering predicts neutron-star radii at the order-of-magnitude level.

Takeaway

Course arc (Lectures 1–6).

- **1–3:** Nuclear size and density (fm, saturation).
- **4–5:** Binding energy, SEMF, most stable Z, mass parabolas.
- **6:** Extreme SEMF: pure neutrons + gravity $\Rightarrow$ neutron-star mass/radius order of magnitude, with pointers to β equilibrium and TOV structure.

Next (Lecture 7). Leave the macroscopic star and return to the microscopic force that underlies a_V: the two-nucleon problem and the deuteron, the only bound NN system.

1.9 Deeper physics: from SEMF cartoon to realistic neutron stars

The pure-neutron SEMF+gravity estimate recovers solar-mass and ten-kilometre scales, but it is not a structure calculation. Three further layers make the cartoon honest without leaving the spirit of this course.

1.9.1 Chemical equilibrium and the proton fraction

In a neutron-star core, weak interactions maintain

$$n \leftrightarrow p + e^- + \bar{\nu}_e \tag{1.19}$$

in equilibrium with charge neutrality $n_p = n_e$ (and muons once $\mu_e > m_\mu c^2$). Chemical equilibrium requires

$$\mu_n = \mu_p + \mu_e. \tag{1.20}$$

Near saturation one may parameterise the energy per nucleon of asymmetric matter as

$$\frac{E}{A} = \varepsilon_0(n_b) + S(n_b)\,(1 - 2x_p)^2 + \cdots\,, \tag{1.21}$$

with proton fraction $x_p = n_p/n_b$ and symmetry energy $S(\rho)$. Differentiating and imposing (1.20) with ultra-relativistic electrons ($\mu_e = \hbar c\,(3\pi^2 n_e)^{1/3}$) yields a few-percent x_p near n_0: matter is neutron rich but not pure neutron. The SEMF $Z = 0$ exercise is therefore a pedagogical limit, not a literal composition. The asymmetry energy still sets the energy cost of that neutron richness: the same a_a (and its density dependence) that shaped the valley of stability controls the pressure of neutron-star matter [4, 1].

1.9.2 Fermi gas: momentum, energy, and degeneracy pressure

In a volume V the number of neutron spin states with momentum less than p_F is

$$N = 2 \cdot \frac{V}{(2\pi\hbar)^3} \cdot \frac{4\pi}{3} p_F^3 = \frac{V p_F^3}{3\pi^2\hbar^3}. \tag{1.22}$$

Hence

$$p_F = \hbar(3\pi^2 n)^{1/3}, \qquad n = N/V. \tag{1.23}$$

At nuclear saturation density $n \approx n_0 \approx 0.16\,\mathrm{fm}^{-3}$,

$$p_F c \approx \hbar c\,(3\pi^2 n_0)^{1/3} \sim 300\,\mathrm{MeV},$$

so the neutrons are mildly relativistic. In the nonrelativistic limit the kinetic energy density and pressure of a Fermi gas are

$$\varepsilon_{\text{kin}} = \frac{3}{5}\, n\, \frac{p_F^2}{2m_n}, \tag{1.24}$$

$$P = \frac{2}{3}\, \varepsilon_{\text{kin}} = \frac{(3\pi^2)^{2/3}}{5} \frac{\hbar^2}{m_n}\, n^{5/3}. \tag{1.25}$$

The corresponding mean degeneracy energy per neutron is

$$\frac{E_{\text{deg}}^{\text{NR}}}{N} = \frac{3}{5} \frac{p_F^2}{2m_n}, \qquad E_{\text{deg}}^{\text{NR}} = \frac{3\alpha^2\hbar^2}{10m_n} \frac{N^{5/3}}{R^2}, \quad \alpha \equiv \left(\frac{9\pi}{4}\right)^{1/3}, \tag{1.26}$$

where $n = 3N/(4\pi R^3)$. Thus the chain is explicit:

$$n \longrightarrow p_F = \hbar(3\pi^2 n)^{1/3} \longrightarrow E_{\text{deg}}^{\text{NR}} \longrightarrow P_{\text{deg}}^{\text{NR}} \propto n^{5/3}.$$

In the ultra-relativistic limit, the filled Fermi sphere instead gives

$$\frac{E_{\text{deg}}^{\text{UR}}}{N} = \frac{3}{4} p_F c, \qquad E_{\text{deg}}^{\text{UR}} = \frac{3\alpha\hbar c}{4} \frac{N^{4/3}}{R}, \qquad P_{\text{deg}}^{\text{UR}} = \frac{1}{3}\varepsilon_{\text{kin}} \propto n^{4/3}. \tag{1.27}$$

These are ideal-gas **toy EOS limits**; interactions are essential near and above saturation density.

That kinetic pressure supports the star against gravity (analogous to electron degeneracy in white dwarfs, but with the neutron mass and nuclear densities). Nuclear potentials modify both energy and pressure: attractive at low density, repulsive at high density. The SEMF volume and asymmetry terms are bulk averages of that physics near n_0; they are not a substitute for $P(\varepsilon)$. Pure neutron matter is not self-bound at zero pressure in realistic calculations: stellar gravity and the EOS together make the compact object.

1.9.3 Energy minimisation and the equilibrium scale

For the same uniform sphere, combine Equation (1.26) with $U_G = -3Gm_n^2 N^2/(5R)$:

$$E_{\text{toy}}^{\text{NR}}(R) = \frac{3\alpha^2\hbar^2}{10m_n} \frac{N^{5/3}}{R^2} - \frac{3Gm_n^2}{5} \frac{N^2}{R}. \tag{1.28}$$

The stationary condition $\mathrm{d}E/\mathrm{d}R = 0$ gives

$$R_{\text{eq}}^{\text{NR}} = \frac{\alpha^2\hbar^2}{Gm_n^3}\, N^{-1/3}. \tag{1.29}$$

Equivalently, the virial relation is $2E_{\text{deg}}^{\text{NR}} + U_G = 0$. Pauli energy rising as R^{-2} therefore balances gravity rising as R^{-1}.

In the ultra-relativistic limit both terms scale as R^{-1}:

$$E_{\text{toy}}^{\text{UR}}(R) = \frac{1}{R}\left[\frac{3\alpha\hbar c}{4} N^{4/3} - \frac{3Gm_n^2}{5} N^2\right]. \tag{1.30}$$

There is no finite-radius minimum in this idealised Newtonian limit. The coefficient changes sign at

$$N_{\text{crit}}^{2/3} = \frac{5\alpha\hbar c}{4Gm_n^2}, \tag{1.31}$$

which exposes a limiting mass scale. Nuclear interactions and general relativity determine the actual stellar sequence.

1.9.4 Hydrostatic equilibrium: Newtonian then TOV

Global binding does not replace local force balance. In Newtonian gravity a spherical shell of thickness $\mathrm{d}r$ is in equilibrium when the pressure gradient balances the gravitational force on the enclosed mass $m(r)$:

$$\frac{\mathrm{d}P}{\mathrm{d}r} = -\frac{Gm(r)\,\rho(r)}{r^2}, \qquad \frac{\mathrm{d}m}{\mathrm{d}r} = 4\pi r^2\rho(r). \tag{1.32}$$

In general relativity the structure of a static spherical star obeys the Tolman–Oppenheimer–Volkoff (TOV) equations. With energy density $\varepsilon(r)$ (including rest mass) and pressure $P(r)$,

$$\frac{\mathrm{d}P}{\mathrm{d}r} = -\frac{G}{c^2}\frac{(\varepsilon + P)(m + 4\pi r^3 P/c^2)}{r^2(1 - 2Gm/(rc^2))}, \tag{1.33}$$

$$\frac{\mathrm{d}m}{\mathrm{d}r} = 4\pi r^2\,\frac{\varepsilon}{c^2}. \tag{1.34}$$

Compared with (1.32), three relativistic corrections appear:

1. $\varepsilon + P$ replaces ρc^2 (pressure gravitates);
2. $m + 4\pi r^3 P/c^2$ replaces m (pressure contributes to the enclosed source);
3. the redshift factor $1 - 2Gm/(rc^2)$ in the denominator steepens the gradient near the Schwarzschild scale.

Boundary conditions: regular centre $m(0) = 0$, $P(0) = P_c$; the stellar surface is the radius R where $P(R) = 0$, and the gravitational mass is $M = m(R)$. The input is a cold equation of state $P(\varepsilon)$; the output is a mass–radius curve $M(R)$ and a maximum mass. Observed $M_{\max} \gtrsim 2\,M_\odot$ pulsars require a sufficiently stiff EOS at a few times ρ_0; GW170817 tidal deformability requires that the EOS not be too stiff near $2\rho_0$. The liquid-drop estimate $R \sim 10\,\text{km}$, $M \sim M_\odot$ is the right order of magnitude; precision astrophysics needs the full EOS ladder [4].

The Newtonian equation is recovered when

$$P \ll \varepsilon, \qquad \varepsilon \simeq \rho c^2, \qquad \frac{2Gm}{rc^2} \ll 1, \qquad \frac{4\pi r^3 P}{mc^2} \ll 1.$$

Then Equation (1.33) reduces to $\mathrm{d}P/\mathrm{d}r = -Gm\rho/r^2$, and Equation (1.34) reduces to $\mathrm{d}m/\mathrm{d}r = 4\pi r^2\rho$.

Key idea

Three layers of understanding.

1. SEMF + gravity: order-of-magnitude A, M, R (this lecture).
2. Fermi gas + β equilibrium: composition and degeneracy pressure.

3. Realistic EOS + TOV: precision $M(R)$, maximum mass, tides.

This course develops layers 1–2 with honest pointers to layer 3.

1.9.5 Link to laboratory symmetry energy

The slope of the symmetry energy $S(\rho)$ at saturation,

$$L = 3n_0 \frac{\mathrm{d}S}{\mathrm{d}n_b}\Big|_{n_0}, \tag{1.35}$$

correlates with the neutron-skin thickness of ^{208}Pb and with neutron-star radii. Lecture 1's charge radii plus parity-violating electron scattering (PREX/CREX) therefore constrain the same physics that sets R_{NS} [1].

1.10 Physics depth: neutron-star mass and radius scales

Lecture 6 recovered the kilometre / solar-mass scale from Newtonian gravity plus nuclear saturation. The argument is robust enough to survive general relativity at the factor-of-two level and fragile enough that the dense-matter EOS still moves radii by kilometres.

1.10.1 Worked estimate: uniform-density star

For constant density ρ and mass $M = (4\pi/3)R^3\rho$, the Newtonian estimate $GM^2/R \sim (M/m_N)\,E_{\mathrm{nuc}}$ with $E_{\mathrm{nuc}} \sim 10\,\mathrm{MeV}$ yields $R \sim 10\,\mathrm{km}$ for $M \sim M_\odot$. Replacing the energy scale by the Fermi energy of a pure neutron gas at n_0 gives the same order. The lesson is dimensional: nuclear density times solar mass must produce kilometres.

$$R \sim \left(\frac{3M}{4\pi m_N n_0}\right)^{1/3} \sim 12\,\mathrm{km} \quad \text{for} \quad M = 1.4\,M_\odot. \tag{1.36}$$

Key idea

What the estimate cannot do. It cannot predict tidal deformability, maximum mass, or a possible phase transition in the core. Those require an EOS $P(\varepsilon)$ integrated in the TOV equations. Laboratory n_0, K, and L anchor only the low-density part of that EOS.

Remark

Assumptions. Newtonian gravity, uniform density, and a single nuclear energy scale. Real stars have crusts, density gradients, and possible exotic cores. Use the estimate to sanity-check published M–R curves, not to replace them.

1.10.2 Crust versus core scales

The outer crust is a lattice of nuclei immersed in electrons; densities climb from terrestrial solids to $\sim 10^{11}\,\mathrm{g\,cm^{-3}}$ before neutrons drip. The inner crust adds a neutron gas. Only above $\sim 0.5\,n_0$ does uniform matter take over. Radius measurements are sensitive to both the crust thickness (correlated with L) and the core stiffness. A change of 1 km in radius at fixed mass is a major nuclear-physics statement, not a small correction.

Maximum masses $\gtrsim 2\,M_\odot$ require a sufficiently stiff core EOS. Softening from hyperons or a phase transition must still allow those masses, which is a strong filter on exotic models. The Lecture 6 dimensional estimate explains why the numbers are kilometres and solar masses; it does not explain why some EOS families are already ruled out.

Convert nuclear saturation density into $2.8 \times 10^{14}\,\mathrm{g\,cm^{-3}}$ and compare with white-dwarf central densities: the gap of several orders of magnitude is why neutron stars require nuclear physics while white dwarfs are still atomic/ionic. Also estimate the Newtonian binding energy GM^2/R for $1.4\,M_\odot$, 12 km: it is a few times 10^{53} erg, comparable to a core-collapse neutrino burst energy scale, linking the structure lecture to multimessenger astrophysics.

Worked compactness

Compute $GM/(Rc^2)$ for $M = 1.4\,M_\odot$ and $R = 11, 12, 13\,\mathrm{km}$. The dimensionless compactness changes by $\sim 10\%$ across that radius range, enough to move tidal deformabilities substantially. This arithmetic shows why radius uncertainties of 1 km are scientifically decisive even though the Lecture 6 scale estimate only aimed at order-of-magnitude kilometres.

Physics-depth close

Dimensional analysis explains why neutron stars are kilometres in radius and solar masses in mass. Nuclear physics enters by fixing n_0 and the EOS stiffness that move those numbers by $\mathcal{O}(1)$, which is exactly the precision multimessenger astronomy now demands.

1.11 Further physics: nuclear density as the NS density scale

Electron scattering yields a bulk nucleon number density and corresponding mass density

$$n_0 \approx 0.16\,\mathrm{fm^{-3}}, \qquad \rho_0 = m_n n_0 \approx 2.68 \times 10^{14}\,\mathrm{g\,cm^{-3}} \tag{1.37}$$

[14, 1]. A self-gravitating ball of that density with mass $M \sim M_\odot$ has radius

$$R \sim \left(\frac{3M}{4\pi\rho_0}\right)^{1/3} \sim 10\text{–}15\,\mathrm{km}, \tag{1.38}$$

the same order obtained from $R = r_0 A^{1/3}$ with $A \sim 10^{57}$. Thus the laboratory saturation density is the bridge between fermi-scale nuclear physics and kilometre-scale compact stars. Realistic neutron-star models replace the pure-neutron SEMF cartoon by β-equilibrated matter and the TOV equation, but they still pass near ρ_0 in the outer core [14, 4].

1.11.1 Drip lines and pure neutrons

The neutron drip line is where $S_n = 0$. Pure neutron matter ($Z = 0$) lies far beyond that line for any laboratory A: the asymmetry energy costs $\sim a_\mathrm{a} \approx 23\,\mathrm{MeV}$ per nucleon relative to $N = Z$

matter, while volume attraction is only $\sim 16\,\mathrm{MeV}$ net. Gravity at $A \sim 10^{57}$ supplies an extra bulk binding $\propto A^{5/3}/R$ that laboratory nuclei never feel [14, 4].

Compact-star densities still pass near the laboratory saturation number density $n_0 \sim 0.16\,\mathrm{fm}^{-3}$ in the outer core; that is why electron-scattering radii and neutron-star radii are conceptually linked.

1.11.2 Gravitational scale and Schwarzschild comparison

For $M = M_\odot$ the Schwarzschild radius is

$$R_\mathrm{S} = \frac{2GM}{c^2} \approx 3\,\mathrm{km}. \tag{1.39}$$

Observed neutron-star radii $\sim$ 10–14 km are only a few times R_S: general relativity is essential for the structure equations, even though the pedagogical SEMF+gravity estimate of this lecture is Newtonian. White dwarfs, supported by electron degeneracy at much lower density, have $R \sim R_\oplus$ and weaker relativity; the larger critical mass scale for neutron stars reflects the larger Fermi energy of nucleons compared with electrons at white-dwarf densities [14].

1.11.3 Asymmetry energy and the crust

In the outer crust of a neutron star, nuclei coexist with a degenerate electron gas; as density rises, nuclei become more neutron rich until free neutrons drip out ($S_n \to 0$). That threshold is the same drip-line physics as in the laboratory SEMF, now under pressure and in β equilibrium. The bulk asymmetry coefficient a_a and the density dependence of the symmetry energy control the proton fraction in the core and the thickness of the crust: links between nuclear mass fits and compact-star observables [14, 4].

1.11.4 Fermi energy in neutron matter

At $n \sim n_0$, a pure neutron gas would have a Fermi energy of order tens of MeV (comparable to the laboratory ε_F scale of Lecture 2). β equilibrium $n \leftrightarrow p + e + \bar{\nu}_e$ then fixes a small proton fraction so that $\mu_n = \mu_p + \mu_e$. The SEMF asymmetry term is a schematic way of writing the cost of $N \neq Z$; modern equations of state refine that cost as a function of density, but the order of magnitude is set by the same nuclear saturation physics measured on Earth.

1.12 Deeper reading: from SEMF to stellar pressure

In the crust, nuclei from Lectures 4–5 coexist with a degenerate electron gas; the neutron drip line appears when S_n hits zero. In the outer core, uniform npe matter takes over, and the pressure is dominated by neutron degeneracy plus interactions. The symmetry energy slope L raises the pressure of neutron-rich matter just above n_0, correlating with both neutron skins (Lecture 1) and stellar radii.

1.12.1 Multimessenger checklist

When reading a mass–radius posterior, ask three nuclear questions: (1) Was n_0 fixed to laboratory saturation? (2) How was L constrained (skins, dipole polarisability, heavy-ion flow)? (3) Is the high-density extension nucleonic or does it allow a phase transition? Gravitational-wave tidal deformability and X-ray pulse-profile radii answer astrophysical questions; they do not erase the need for those nuclear anchors. Lectures 23–24 later remind us that the same nuclei can also fission when assembled in terrestrial or astrophysical extremes.

1.12.2 Laboratory anchors checklist

Useful laboratory anchors include: saturation density and binding from masses and radii; incompressibility from giant resonances; symmetry energy and its slope from skins, dipole polarisability, and heavy-ion flow; high-density constraints from hard photon or meson production (more model dependent). Astrophysical anchors include pulsar masses, NICER radii, and GW170817 tidal deformability. A responsible EOS paper states which anchors were imposed as priors and which were used only as posterior checks.

Convert nuclear saturation density into $2.8 \times 10^{14}\,\mathrm{g\,cm^{-3}}$ and compare with white-dwarf central densities: the gap of several orders of magnitude is why neutron stars require nuclear physics while white dwarfs are still atomic/ionic. Also estimate the Newtonian binding energy GM^2/R for $1.4\,M_\odot$, $12\,\mathrm{km}$: it is a few times $10^{53}\,\mathrm{erg}$, comparable to a core-collapse neutrino burst energy scale, linking the structure lecture to multimessenger astrophysics.

Neutron-star checklist

(1) Convert n_0 to $\mathrm{g\,cm^{-3}}$. (2) Estimate uniform-density R for $1.4\,M_\odot$. (3) List laboratory anchors (n_0, K, L) separately from astrophysical anchors (masses, radii, tides). (4) State whether a published EOS allows a phase transition. This checklist prevents treating a multimessenger posterior as if it had no nuclear priors.

Tidal deformability intuition

For a given mass, a larger radius usually implies a larger tidal deformability Λ, because the star is less compact. Soft EOS families that shrink radii also suppress Λ, which is why GW170817's tidal constraint reshaped the nuclear EOS landscape alongside radius measurements. The Lecture 6 dimensional estimate cannot predict Λ, but it explains why the relevant compactness $GM/(Rc^2)$ is $\mathcal{O}(0.15)$ rather than planetary.

Crust thickness and L

A larger symmetry-energy slope L typically thickens the crust and increases the radius at fixed mass for many EOS parametrisations. Neutron skins of $^{208}\mathrm{Pb}$ correlate with that slope. Laboratory skins and astrophysical radii are therefore not independent anecdotes; they are linked through the same isovector physics introduced in Lectures 1–2.

Reading an M–R curve

On a published mass–radius plot, mark $1.4\,M_{\odot}$ and read off radius ranges for soft and stiff EOS bands. Convert the radius difference into a compactness difference. Then ask which nuclear priors (n_0, K, L) were imposed. If the paper does not say, the posterior is harder to interpret for nuclear physics purposes even if the astrophysics is carefully done.

Neutron stars convert nuclear saturation into astrophysical kilometres. Keeping laboratory anchors and multimessenger observables on separate mental lists is the clearest way to read contemporary EOS papers without confusion.

In practice, rework one numerical estimate from the lecture with a different parameter set and compare the shift to the quoted experimental uncertainty. If the shift exceeds the uncertainty, the estimate is teaching a scale, not delivering a fit. That distinction keeps theoretical cartoons honest when they sit beside evaluated data tables and modern many-body calculations. Along the course arc, write one sentence linking this chapter backward and one forward: the discipline of those two sentences is as important as any single formula. Examination problems rarely ask for a literature review, but they do ask for the scale argument that literature reviews presuppose.

Research frontier: multimessenger neutron-star EOS and student projects

Lecture 6 used Newtonian gravity and SEMF bookkeeping to recover the kilometre/solar-mass scale of neutron stars. That estimate remains an excellent order-of-magnitude check, but quantitative astrophysics now combines general relativistic structure equations with laboratory nuclear constraints. Since GW170817, tidal deformability from gravitational waves, NICER pulse-profile radii, and massive pulsars jointly constrain the dense-matter equation of state, while laboratory symmetry-energy and neutron-skin data supply the low-density anchor [47, 46, 45, 38]. Whether the core contains only nucleonic matter or hosts a phase transition (hyperons, quark matter, or condensates) remains unsettled; the Bayesian combination of laboratory and astrophysical likelihoods is a major research industry. Uncertainties that still dominate EOS posteriors include the high-density symmetry energy, the possible presence of first-order phase transitions, and systematic modelling of the neutron-star crust. The pedagogical lesson of the lecture survives: without nuclear saturation density and a stiffness measure near and above n_0, even the most precise multimessenger data cannot be interpreted.

A clean student project is to hold the low-density nuclear constraints fixed and vary only the high-density extension, then ask which multimessenger observable moves. That exercise makes the division of labour between laboratory nuclear physics and astrophysical inference explicit, and it shows why PREX, NICER, and GW170817 are complementary rather than redundant.

Student directions. (1) Analytic estimate: recompute the uniform-density radius $R = r_0 A^{1/3}$ for $A = 10^{57}$ and compare with a published $1.4\,M_{\odot}$ radius range. (2) Conceptual link: relate PREX's L constraint qualitatively to crust thickness and tidal deformability. (3) Term paper: compare GW170817 tidal limits with NICER radius posteriors, citing at least one review [46].

1.13 Problems with solutions

Problem 6.1 — Nucleon number of a solar-mass neutron star

Estimate A for a neutron star of mass $M = 1.4\,M_\odot$ ($M_\odot = 2\times10^{30}$ kg, $m_n = 1.67\times10^{-27}$ kg).

Solution 6.1

$$A \approx \frac{M}{m_n} = \frac{1.4\times2\times10^{30}}{1.67\times10^{-27}} = \frac{2.8\times10^{30}}{1.67\times10^{-27}} \approx 1.7\times10^{57}.$$

Order of magnitude: $A \sim 10^{57}$.

Problem 6.2 — Radius from nuclear density (Petrera 1.1.3)

Convert $n_0 = 0.16\,\mathrm{fm}^{-3}$ to mass density using $m_n = 1.6749\times10^{-27}$ kg. Then use that density and $M = M_\odot$, recompute R and compare with $R = r_0A^{1/3}$ for $A = M/m_n$, where $r_0 = (3/4\pi n_0)^{1/3}$.

Solution 6.2

The conversion is

$$\rho_0 = m_n n_0 = (1.6749\times10^{-27})(0.16\times10^{45}) = 2.68\times10^{17}\,\mathrm{kg\,m^{-3}} = 2.68\times10^{14}\,\mathrm{g\,cm^{-3}}.$$

From density:

$$R = \left(\frac{3M}{4\pi\rho}\right)^{1/3} = \left(\frac{3\times2\times10^{33}\,\mathrm{g}}{4\pi\times2.68\times10^{14}\,\mathrm{g\,cm^{-3}}}\right)^{1/3} \approx 12.1\,\mathrm{km}.$$

(cf. Problem 2.2). Also

$$A = \frac{M_\odot}{m_n} \approx 1.19\times10^{57}, \qquad r_0 = \left(\frac{3}{4\pi n_0}\right)^{1/3} \approx 1.14\,\mathrm{fm}.$$

Therefore

$$R = 1.14\,\mathrm{fm}\times(1.19\times10^{57})^{1/3} = 12.1\,\mathrm{km}.$$

The two expressions agree identically because r_0 was derived from the same uniform density.

Problem 6.3 — SEMF pure neutrons unbound

With $a_V = 15.5$ MeV and $a_a = 23$ MeV, show that pure neutron matter ($Z = 0$) has negative binding per nucleon from nuclear terms alone, and estimate the critical A at which $CA^{2/3}$ with $C = 3Gm_n^2/(5r_0) \sim 6\times10^{-37}$ MeV can compensate.

Solution 6.3

For $Z = 0$, $N = A$,

$$\frac{B}{A} \approx a_V - a_\mathrm{a} = 15.5 - 23 = -7.5\,\mathrm{MeV}$$

(unbound). Adding the gravity piece $+CA^{2/3}$ per nucleon and setting $CA^{2/3} = 7.5\,\mathrm{MeV}$,

$$A^{2/3} = \frac{7.5}{6 \times 10^{-37}} \sim 1.3 \times 10^{37}, \qquad A \sim (1.3 \times 10^{37})^{3/2} \sim 10^{56}.$$

This is the stellar scale of Lecture 6. (The precise C comes from $3GM^2/(5R)$ with $M = Am_n$, $R = r_0 A^{1/3}$.)

Problem 6.4 — Fermi momentum at saturation

Using $p_F = \hbar(3\pi^2 n)^{1/3}$ and $n = n_0 = 0.16\,\mathrm{fm}^{-3}$, compute $p_F c$ in MeV and comment on whether the neutrons are nonrelativistic.

Solution 6.4

$$(3\pi^2 n)^{1/3} = \left(3\pi^2 \times 0.16\right)^{1/3} \approx (4.74)^{1/3} \approx 1.68\,\mathrm{fm}^{-1},$$
$$p_F c = \hbar c \cdot 1.68 \approx 197 \times 1.68 \approx 330\,\mathrm{MeV}.$$

Since $m_n c^2 \approx 940\,\mathrm{MeV}$, one has $p_F c/(m_n c^2) \sim 0.35$: mildly relativistic. The nonrelativistic pressure formula is a first estimate; a realistic EOS must include relativistic kinematics and nuclear interactions.

Problem 6.5 — Degeneracy–gravity balance

For N neutrons in a uniform sphere, use $p_F = \alpha\hbar N^{1/3}/R$, $\alpha = (9\pi/4)^{1/3}$. (a) Derive the nonrelativistic degeneracy energy and minimise $E = E_\mathrm{deg} - 3Gm_n^2 N^2/(5R)$. (b) Show why the ultra-relativistic limit produces a limiting mass rather than a finite equilibrium radius in this toy model.

Solution 6.5

The filled Fermi sphere has mean kinetic energy $3p_F^2/(10m_n)$, hence

$$E_\mathrm{deg}^\mathrm{NR} = \frac{3\alpha^2\hbar^2}{10m_n}\frac{N^{5/3}}{R^2}.$$

Setting $\mathrm{d}E/\mathrm{d}R = 0$ gives

$$R_\mathrm{eq} = \frac{\alpha^2\hbar^2}{Gm_n^3}N^{-1/3}, \qquad 2E_\mathrm{deg}^\mathrm{NR} + U_G = 0.$$

Ultra-relativistically,

$$E_{\text{deg}}^{\text{UR}} = \frac{3\alpha\hbar c}{4}\frac{N^{4/3}}{R},$$

so both kinetic and gravitational terms scale as R^{-1}. Their coefficients determine stability; equality gives $N_{\text{crit}}^{2/3} = 5\alpha\hbar c/(4Gm_n^2)$. A realistic maximum mass requires interactions and TOV gravity.

Bibliography

[1] R. A. Dunlap, *An Introduction to the Physics of Nuclei and Particles* (2nd ed.), IOP Publishing, Bristol (2023), DOI: 10.1088/978-0-7503-6094-4, Ch. 3 (Nuclear composition and size).

[2] W. Demtröder, *Nuclear and Particle Physics*, Undergraduate Lecture Notes in Physics, Springer, Cham (2023).

[3] S. Petrera, *Problems and Solutions in Nuclear and Particle Physics*, UNITEXT for Physics, Springer, Cham (2019).

[4] F. Terranova, *A Modern Primer in Particle and Nuclear Physics*, Oxford University Press (2021).

[5] S. D'Auria, *Introduction to Nuclear and Particle Physics*, Undergraduate Lecture Notes in Physics, Springer, Cham (2018).

[6] K. S. Krane, *Introductory Nuclear Physics*, Wiley, New York (1988).

[7] R. Hofstadter, "Electron scattering and nuclear structure," Rev. Mod. Phys. **28**, 214 (1956).

[8] H. F. Ehrenberg, R. Hofstadter, U. Meyer-Berkhout, D. G. Ravenhall, and S. E. Sobottka, "High-Energy Electron Scattering and the Charge Distribution of Carbon-12 and Oxygen-16," Phys. Rev. **113**, 666 (1959).

[9] H. Yukawa, "On the interaction of elementary particles. I," Proc. Phys.-Math. Soc. Japan **17**, 48 (1935).

[10] R. D. Woods and D. S. Saxon, "Diffuse surface optical model for nucleon-nuclei scattering," Phys. Rev. **95**, 577 (1954).

[11] H. G. J. Moseley, "The high-frequency spectra of the elements," Phil. Mag. **26**, 1024 (1913); **27**, 703 (1914).

[12] C. F. von Weizsäcker, "Zur Theorie der Kernmassen," Z. Phys. **96**, 431 (1935).

[13] P. Cappellaro, *Introduction to Applied Nuclear Physics* (MIT OpenCourseWare / LibreTexts), CC BY-NC-SA 4.0.

[14] J.-L. Basdevant, J. Rich, and M. Spiro, *Fundamentals in Nuclear Physics: From Nuclear Structure to Cosmology*, Springer, New York (2005).

[15] D. Tong, *Particle Physics*, Lecture notes (University of Cambridge / CERN school notes).

[16] M. G. Mayer, "On closed shells in nuclei. II," Phys. Rev. **75**, 1969 (1949).

[17] O. Haxel, J. H. D. Jensen, and H. E. Suess, "On the "magic numbers" in nuclear structure," Phys. Rev. **75**, 1766 (1949).

[18] T. Schmidt, "Über die magnetischen Momente der Atomkerne," Z. Phys. **106**, 358 (1937).

[19] L. W. Nordheim, "On spins, moments, and shells in nuclei," Phys. Rev. **78**, 294 (1950).

[20] Evaluated Nuclear Structure Data File (ENSDF), National Nuclear Data Center, Brookhaven National Laboratory, `https://www.nndc.bnl.gov/ensdf/`.

[21] NuDat 3, National Nuclear Data Center, Brookhaven National Laboratory, `https://www.nndc.bnl.gov/nudat3/`.

[22] N. J. Stone, "Table of nuclear magnetic dipole and electric quadrupole moments," At. Data Nucl. Data Tables **90**, 75 (2005); updated compilations at NNDC.

[23] W. N. Cottingham and D. A. Greenwood, *An Introduction to Nuclear Physics* (2nd ed.), Cambridge University Press, Cambridge (2001).

[24] H. Geiger and J. M. Nuttall, "The ranges of the α particles from the radioactive substances," Phil. Mag. **22**, 613 (1911).

[25] G. Gamow, "Zur Quantentheorie des Atomkernes," Z. Phys. **51**, 204 (1928).

[26] R. W. Gurney and E. U. Condon, "Wave mechanics and radioactive disintegration," Nature **122**, 439 (1928); Phys. Rev. **33**, 127 (1929).

[27] M. Wang, W. J. Huang, F. G. Kondev, G. Audi, and S. Naimi, "The AME 2020 atomic mass evaluation (II). Tables, graphs and references," Chin. Phys. C **45**, 030003 (2021).

[28] Laboratoire National Henri Becquerel (LNHB), Recommended decay data, `http://www.lnhb.fr/nuclear-data/nuclear-data-table/`.

[29] L. M. Langer, R. D. Moffat, and H. C. Price, Jr., "Low energy beta-ray spectra: P^{32} and Cu^{64}," Phys. Rev. **76**, 1725 (1949).

[30] L. M. Langer and H. C. Price, Jr., "Shapes of the beta-spectra of the forbidden transitions of Sb^{124}, Rb^{86}, Sr^{89}, Y^{91}, and Cs^{137}," Phys. Rev. **75**, 1769 (1949).

[31] D. C. Camp and L. M. Langer, "The shape of the ^{66}Ga positron spectrum and the contribution from $0^+ \to 0^+$ transitions," Phys. Rev. **129**, 1782 (1963).

[32] H. C. Verma, *Nuclear Physics: Fundamentals and Applications*, NPTEL/IIT Kanpur lecture series, `https://hcverma.in/ncl_phy_lectures`.

[33] International Atomic Energy Agency, *LiveChart of Nuclides*, evaluated structure, decay, reaction, and fission-yield data, `https://www-nds.iaea.org/relnsd/vcharthtml/VChartHTML.html`.

[34] T. Kibédi, T. W. Burrows, M. B. Trzhaskovskaya, P. M. Davidson, and C. W. Nestor, Jr., "Evaluation of theoretical conversion coefficients using BrIcc," Nucl. Instrum. Methods Phys. Res. A **589**, 202 (2008), DOI: 10.1016/j.nima.2008.02.051.

[35] D. A. Brown *et al.*, "ENDF/B-VIII.0: The 8th major release of the nuclear reaction data library with CIELO-project cross sections, new standards and thermal scattering data," Nucl. Data Sheets **148**, 1 (2018), DOI: 10.1016/j.nds.2018.02.001.

[36] B. Acharya *et al.*, "Solar fusion III: New data and theory for hydrogen-burning stars," Rev. Mod. Phys. **97**, 035002 (2025), DOI: 10.1103/8lm7-gs18.

[37] S. N. Ghoshal, "An experimental verification of the theory of compound nucleus," Phys. Rev. **80**, 939 (1950), DOI: 10.1103/PhysRev.80.939.

[38] D. Adhikari *et al.* (PREX Collaboration), "Accurate determination of the neutron skin thickness of ^{208}Pb through parity-violation in electron scattering," Phys. Rev. Lett. **126**, 172502 (2021), DOI: 10.1103/PhysRevLett.126.172502.

[39] B. T. Reed, F. J. Fattoyev, C. J. Horowitz, and J. Piekarewicz, "Implications of PREX-II on the equation of state of neutron-rich matter," Phys. Rev. Lett. **126**, 172503 (2021), DOI: 10.1103/PhysRevLett.126.172503.

[40] B. Hu *et al.*, "Ab initio predictions link the neutron skin of ^{208}Pb to nuclear forces," Nature Phys. **18**, 1196 (2022), DOI: 10.1038/s41567-022-01715-8.

[41] E. Epelbaum, H.-W. Hammer, and U.-G. Meißner, "Modern theory of nuclear forces," Rev. Mod. Phys. **81**, 1773 (2009), DOI: 10.1103/RevModPhys.81.1773.

[42] H.-W. Hammer, S. König, and U. van Kolck, "Nuclear effective field theory: Status and perspectives," Rev. Mod. Phys. **92**, 025004 (2020), DOI: 10.1103/RevModPhys.92.025004.

[43] T. Otsuka, A. Gade, O. Sorlin, T. Suzuki, and Y. Utsuno, "Evolution of shell structure in exotic nuclei," Rev. Mod. Phys. **92**, 015002 (2020), DOI: 10.1103/RevModPhys.92.015002.

[44] H. Hergert, S. K. Bogner, T. D. Morris, A. Schwenk, and K. Tsukiyama, "The in-medium similarity renormalization group: A novel ab initio method for nuclei," Phys. Rep. **621**, 165 (2016), DOI: 10.1016/j.physrep.2015.12.007.

[45] J. M. Lattimer and M. Prakash, "The equation of state of hot, dense matter and neutron stars," Phys. Rep. **621**, 127 (2016), DOI: 10.1016/j.physrep.2015.12.005.

[46] J. M. Lattimer, "Neutron stars and the nuclear matter equation of state," Annu. Rev. Nucl. Part. Sci. **71**, 433 (2021), DOI: 10.1146/annurev-nucl-102419-124827.

[47] B. P. Abbott *et al.* (LIGO Scientific Collaboration and Virgo Collaboration), "GW170817: Observation of gravitational waves from a binary neutron star inspiral," Phys. Rev. Lett. **119**, 161101 (2017), DOI: 10.1103/PhysRevLett.119.161101.

[48] M. J. Dolinski, A. W. P. Poon, and W. Rodejohann, "Neutrinoless double-beta decay: Status and prospects," Annu. Rev. Nucl. Part. Sci. **69**, 219 (2019), DOI: 10.1146/annurev-nucl-101918-023407.

[49] M. Agostini, G. Benato, J. A. Detwiler, J. Menéndez, and F. Vissani, "Toward the discovery of matter creation with neutrinoless $\beta\beta$ decay," Rev. Mod. Phys. **95**, 025002 (2023), DOI: 10.1103/RevModPhys.95.025002.

[50] P. Gysbers *et al.*, "Discrepancy between experimental and theoretical β-decay rates resolved from first principles," Nature Phys. **15**, 428 (2019), DOI: 10.1038/s41567-019-0450-7.

[51] H. L. Crawford, K. Fossez, S. König, and A. Spyrou, "A vision for the science of rare isotopes," Annu. Rev. Nucl. Part. Sci. **74**, 141 (2024), DOI: 10.1146/annurev-nucl-121423-091501.

[52] Nuclear Science Advisory Committee, *A New Era of Discovery: The 2023 Long Range Plan for Nuclear Science*, U.S. Department of Energy and National Science Foundation (2023), `https://nuclearsciencefuture.org/`.

[53] S. A. Giuliani, Z. Matheson, W. Nazarewicz, E. Olsen, P.-G. Reinhard, J. Sadhukhan, B. Schuetrumpf, N. Schunck, and P. Schwerdtfeger, "Colloquium: Superheavy elements: Oganesson and beyond," Rev. Mod. Phys. **91**, 011001 (2019), DOI: 10.1103/RevModPhys.91.011001.

[54] N. Schunck and D. Regnier, "Theory of nuclear fission," Prog. Part. Nucl. Phys. **125**, 103963 (2022), DOI: 10.1016/j.ppnp.2022.103963.

[55] I. Counts, J. Hur, D. P. L. Aude Craik, H. Jeon, C. Leung, J. C. Berengut, A. Geddes, A. Kawasaki, W. Jhe, and V. Vuletić, "Evidence for nonlinear isotope shift in Yb^+ search for new boson," Phys. Rev. Lett. **125**, 123002 (2020), DOI: 10.1103/PhysRevLett.125.123002.

[56] I. Angeli and K. P. Marinova, "Table of experimental nuclear ground state charge radii: An update," At. Data Nucl. Data Tables **99**, 69 (2013), DOI: 10.1016/j.adt.2011.12.006.

[57] S. Kraemer *et al.*, "Observation of the radiative decay of the ^{229}Th nuclear clock isomer," Nature **617**, 706 (2023), DOI: 10.1038/s41586-023-05894-z.